Study of Base Pressure in Laminar Hypersonic Flow: Re-entry Flight Measurements

Bruce M. Bulmer*
Sandia Laboratories, Albuquerque, N. Mex.

Base pressure data from flight tests of four full-scale re-entry vehicles are analyzed. The flight vehicles were nearly identical, slightly blunted, 9° half-angle sphere cones. Flow conditions were hypersonic, $M_\infty \approx 16$-20, and the cone boundary layer and near wake were laminar for Reynolds numbers Re_{∞_L} between 2×10^5 and 5×10^7. The flight data are compared with available theory and ground- and flight-test data for similar configurations. Various correlation parameters, derived from both experimental ground-test and theoretical results, are utilized in this analysis. Suitable data correlations were obtained with the reduced Reynolds number suggested by Wu and Su and with parameters from the Reeves and Buss theory. Correlations of the present data are directed toward establishing a basis for re-entry vehicle preflight predictions and postflight data analyses. Resulting base pressure calculations for other slender configurations (7°, 8°, and 10° cones) in hypersonic entry conditions show good agreement with both theory and flight data and indicate the importance of including real-gas and nose-bluntness effects in high Reynolds-number laminar flows.

Nomenclature

h	= static enthalpy
H	= total enthalpy
L	= axial length of cone
M	= Mach number
p	= static pressure
R	= base radial coordinate
R_B, R_N	= base, nose radius
R_N/R_B	= bluntness ratio
Re	= Reynolds number
Re_c	= reduced Reynolds number, Eq. (1)
s	= wetted length of cone surface
V	= velocity
γ	= ratio of specific heats
θ_c	= cone half-angle
ϕ	= base angular coordinate
Subscripts	
b	= base condition
e	= local cone (boundary-layer edge) condition immediately preceding base at s
L	= based on axial length of cone
R_B	= based on base radius
s	= based on wetted length of cone surface
w	= cone surface (wall) condition immediately preceding base at s
δ	= based on total boundary-layer thickness immediately preceding base at s
θ	= based on boundary-layer momentum thickness immediately preceding base at s
∞	= freestream condition

I. Introduction

THE wake of a slender body in hypersonic flow can be a significant source of observables (electrons and radiating species). As a result, interest in wakes has been motivated, primarily, by the desire to detect and identify (i.e., to discriminate), and to communicate with, bodies entering the atmosphere.[1] Since the downstream (far) wake characteristics of relatively sharp, slender hypersonic bodies are governed, to a large extent, by the separation, recirculation, and recompression processes near the base of the body, the solution of the near wake (or base-flow region), which extends from the base of the body to the neck of the wake, provides appropriate initial conditions required for far-wake computations.

Numerous experimental and theoretical hypersonic near-wake studies appear in the literature.[2-5] One purpose for the investigation of the near wake has been to develop a capability for predicting the base pressure of slender hypersonic re-entry configurations. Certain properties of the near-wake flowfield structure (e.g., temperature distributions in the base-flow region and near-wake pressure, density, and velocity profiles) are significant from the viewpoint of design and development of advanced re-entry vehicle (RV) systems. As a result, while base pressure estimates are required in RV targeting (drag) and afterbody design considerations, the need for determining base pressure generally stems from the fact that the base pressure represents a boundary condition, or starting point, for the solution of the near-wake flowfield of an RV.

Laminar near wakes generally occur in altitude regions that are of current practical interest. For slender hypersonic bodies, a significant portion of the wake remains laminar over a wide range of freestream Reynolds numbers; consequently, the near wake of an RV is usually laminar for the majority of the total altitude history in the continuum flow regime (i.e., below 250 kft). For this case, the near wake is a complicated flow which is, unfortunately, extremely difficult to model analytically. This is evidenced by the increased experimental effort in recent years to help characterize the fluid physics of hypersonic wakes in general. Because the base pressure is essential to the solution of the near-wake recirculating flowfield, methods for determining the base pressure of axisymmetric slender cones in laminar hypersonic flow have received considerable attention.[6-24] In some of these studies,[8,10-14] base pressure data free of support-interference effects were obtained for slightly blunted slender cones and for limited ranges of flow parameters (freestream Mach number M_∞, freestream Reynolds number Re_{∞_l}, wall-to-total-enthalpy ratio h_w/H_∞, etc.). However, complete ground-test simulation of the flight conditions typical of advanced hypersonic RVs is generally not possible. For example, $Re_{\infty_L} \approx 10^5$-$10^8$ and $h_w/H_\infty \approx 0.02$-$0.12$ at $15 < M_\infty < 25$ may be required for flight simulation of laminar near-wake flows under the atmospheric entry conditions of current interest.

Presented as Paper 74-537 at the AIAA 7th Fluid and Plasma Dynamics Conference, Palo Alto, California, June 17-19, 1974; submitted July 1, 1974; revision received February 3, 1975. This work was jointly supported by the U.S. Atomic Energy Commission and the U.S. Air Force Space and Missile Systems Organization.

Index categories: Entry Vehicle Testing; Jets, Wakes, and Viscid-Inviscid Flow Interactions; Supersonic and Hypersonic Flow.

*Member, Technical Staff, Re-entry Vehicle Aerothermodynamics Division. Member AIAA.

While some hypersonic ($M_\infty > 15$) ground-test base pressure data from slender cones are available for correlation purposes, laminar base pressure results from full-scale reentry vehicle flight tests are very limited in the literature. Flight-test data are invaluable and provide both trend information and specific results under operational conditions with which to examine the validity of theoretical approaches and ground-test simulation. Cassanto and Hoyt[25,26] have reported full-scale RV base pressure data at $M_\infty = 20$-22 for several slender flight configurations, and Ohrenberger and Baum[24] briefly discuss some RV flight data to compare with theory at $M_\infty = 21$.

In this paper, laminar hypersonic base pressure data from four recent RV flight tests[27] are presented and discussed. The flight conditions are representative of advanced RV systems (i.e., high M_∞ and Re_{∞_L} and low h_w/H_∞ in laminar flow). Whenever possible, the flight data are compared with available theory and ground- and flight-test data for similar configurations. Analyses of the data utilize several correlation parameters derived from experimental ground-test results as well as from theoretical considerations; correlations of the present data are directed toward establishing a basis for re-entry vehicle preflight predictions and postflight data analyses. Base pressure predictions are developed for other slender configurations and are compared with both theory and flight-test data. A limited parametric study is included to emphasize real-gas and nose-bluntness effects on the base pressure of a slender cone.

II. RV Configurations and Flight Conditions

The flight vehicles were nearly identical slender cones with spherically blunted nosetips and essentially flat base geometry. The bluntness ratio R_N/R_B was 0.05 for Flights 1 and 2 and 0.06 for Flights 3 and 4; all four RVs had a cone half-angle θ_c of 9°. A schematic of the vehicles is presented in Fig. 1.

During the period for which data are presented, the freestream Mach number was relatively constant for each flight: Flights 1 and 2, $M_\infty \approx 16$; Flight 3, $M_\infty \approx 20$; and Flight 4, $M_\infty \approx 19$. Data were analyzed for the range of freestream Reynolds number Re_{∞_L} between 2.5×10^5 and 4.8×10^7. Calculated postflight trajectories that included telemetered RV acceleration data were used in this analysis. Atmospheric conditions were derived from radiosonde data obtained in the high Re_{∞_L} (low altitude) regime, and the appropriate standard atmosphere was utilized in the low Re_{∞_L} (high altitude) regime.

III. Instrumentation

Each RV was instrumented with a low-range transducer designed to provide base pressure measurements during that portion of re-entry for which the cone surface boundary layer was laminar. Two types of transducers were utilized in these tests (refer to Table 1). Instrumentation on Flights 1 and 2 consisted of Metrophysics (MPI) thermal-conductivity transducers (0-50 Torr nominal range). Tavis variable-reluctance

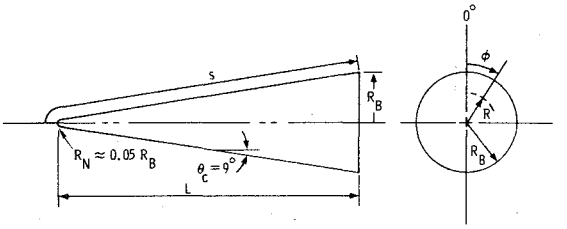

FLT	R_N/R_B	s/L	R_B/L
1	0.05	1.017	0.165
2	0.05	1.017	0.165
3	0.06	1.018	0.167
4	0.06	1.018	0.167

Fig. 1 Re-entry vehicle configuration.

transducers (0-1 psia nominal range) were used on Flights 3 and 4. The MPI sensor had segmented output designed to provide a six-fold increase in sensitivity and thereby to provide accurate pressure measurements to as low as 0.2% of the full-scale transducer output (altitudes in excess of 200 kft). The estimated data uncertainty of the Tavis transducer is ±2% of full scale. In Table 1, the location of each instrument is specified by R, the radial distance from the base centerline, and by ϕ, the base angular coordinate. Note that all transducers were mounted at the same base radial location ($R/R_B = 0.1$).

For Flights 1 and 2, the MPI transducer was isolated from heat, vibration, and shock by mounting on a short section of soft rubber tubing, which in turn was mounted to the pressure-port fitting on the inside of the base cover. The pressure time lag is considered negligible because of the very short pneumatic system between the transducer and the pressure port (tube length/port diameter ratio of 12) and the negligible sensor volume. Because of its size, the Tavis transducer used for Flights 3 and 4 was attached to the pressure-port fitting with 1/8-in. diam rubber tubing approximately 5 in. in length (tube length/port diameter ratio of 40). While this mounting technique increased the pneumatic system length/diameter ratio somewhat, the pressure time lag for Flights 3 and 4 may also be considered negligible in the altitude range of interest.

IV. Flight Test Results

Figure 2 shows the base pressure data, normalized by freestream static pressure, in terms of the freestream Reynolds number. All of the data presented correspond to absolute pressure levels which exceed 1% of the full-scale transducer output for Flights 1 and 2 and 2% for Flights 3 and 4. Onboard thermal instrumentation verified that a completely laminar boundary layer existed on the RV cone surface during the period for which data are presented. In addition, base heat-transfer measurements indicated that the base-flow region was laminar. While the exact history of the movement of transition in the wake is not known, wake transition studies indicate that, for the range of M_∞ and Re_{∞_L} of interest, the

Table 1 Base pressure instrumentation

Flight	Instrument description	Nominal range	Location R/R_B	Location ϕ(deg)	Sampling rate (/sec)
1	Metrophysics (MPI) No. 101Q71 segmented thermal-conductivity type	0-50 Torr, 6 segments	0.1	285	30
2	Metrophysics (MPI) No. 101Q71 segmented thermal-conductivity type	0-50 Torr, 6 segments	0.1	285	30
3	Tavis No. P-1 variable-reluctance type	0-1 psia	0.1	154	15
4	Tavis No. P-1 variable-reluctance type	0-1 psia	0.1	154	15

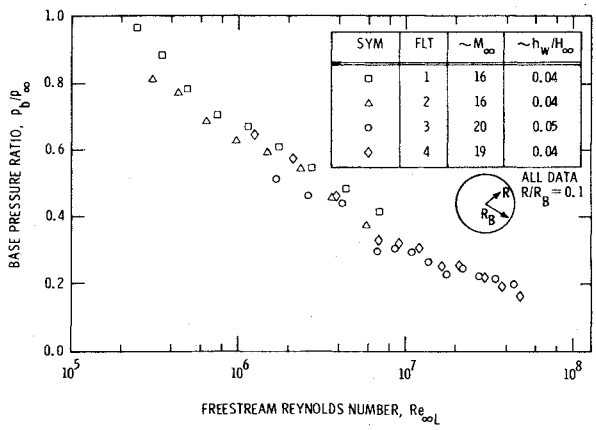

Fig. 2 Flight data: base pressure in laminar flow.

transition point was generally well downstream from the neck of the wake.[28,29] It is known that the movement of transition from the neck region to the body boundary layer of a slightly blunted slender cone has a pronounced effect on the near-wake flowfield and, in particular, on the base pressure.[30,31] However, the consistent variation of p_b/p_∞ with increasing Re_{∞_L} among all of the flights (refer to Fig. 2), together with the onboard thermal instrumentation, confirms that transition did not move onto the body for the Reynolds numbers considered here (transition onset was in fact detected later in each of the flights). Therefore, the entire near-wake region is assumed to be laminar in nature for all of the data shown in Fig. 2.

The angle of attack for the flights was generally 2.5° or less for $Re_{\infty_L} < 10^6$ and damped to 0.5° for $Re_{\infty_L} > 10^7$. Ground-test data[21] for a sharp 10° cone and approximately the same conditions ($M_\infty \approx 19$, $Re_{\infty_L} = 3.7 \times 10^5$ to 1.7×10^6) indicate variations in centerline base pressure from the zero angle-of-attack value of the order of 5% or less for the angle-of-attack range previously noted. Thus, the effect of the small angles of attack is neglected in the analysis of the present data, and the base flow is assumed to be axisymmetric.

A detailed summary of the present data and pertinent flow parameters is given in Table 2; geometrical relationships for each vehicle are provided in Fig. 1 so that other desired parameters (e.g., Re_{eR_B}) may be determined from Table 2. The local cone properties immediately preceding the base (i.e., the boundary-layer edge conditions at s) were determined for the RV configurations and trajectories by an iterative technique[32] in which the laminar boundary layer on

Table 2 Summary of flight data and flow parameters

p_b/p_∞	p_b/p_e	$Re_{\infty_L} \times 10^{-6}$	M_e	$Re_{es} \times 10^{-6}$	$\delta/R_B \times 10^2$	$Re_{e\theta}$	h_w/H_∞
			FLT 1 $M_\infty \approx 16$				
0.965	0.0908	0.247	10.43	0.702	2.19	323	0.034
0.888	0.0852	0.344	10.38	0.978	1.85	379	0.034
0.784	0.0750	0.497	10.31	1.39	1.54	450	0.034
0.707	0.0665	0.739	10.24	2.00	1.28	537	0.035
0.676	0.0622	1.13	10.15	2.92	1.05	645	0.036
0.610	0.0550	1.75	10.00	4.22	0.870	769	0.037
0.547	0.0485	2.73	9.82	6.07	0.718	914	0.038
0.483	0.0422	4.32	9.57	8.66	0.593	1080	0.040
0.418	0.0359	6.89	9.05	11.4	0.512	1220	0.043
			FLT 2 $M_\infty \approx 16$				
0.809	0.0767	0.300	10.42	0.855	1.98	355	0.034
0.769	0.0733	0.427	10.36	1.21	1.66	420	0.035
0.688	0.0650	0.624	10.28	1.72	1.39	499	0.036
0.622	0.0575	0.951	10.21	2.51	1.14	600	0.038
0.595	0.0539	1.47	10.08	3.65	0.939	718	0.040
0.540	0.0480	2.29	9.90	5.27	0.775	856	0.041
0.455	0.0398	3.61	9.69	7.57	0.639	1010	0.043
0.373	0.0321	5.76	9.29	10.4	0.539	1170	0.044
			FLT 3 $M_\infty \approx 20$				
0.512	0.0337	1.64	10.60	3.58	0.927	701	0.031
0.462	0.0298	2.59	10.29	5.02	0.770	817	0.034
0.440	0.0263	4.11	9.65	6.34	0.679	909	0.037
0.296	0.0182	6.79	8.85	7.80	0.608	1000	0.041
0.305	0.0186	8.57	8.45	8.46	0.581	1040	0.043
0.295	0.0181	10.8	8.02	9.06	0.560	1070	0.046
0.264	0.0162	13.7	7.60	9.69	0.541	1110	0.049
0.229	0.0140	17.4	7.20	10.3	0.523	1140	0.052
0.243	0.0150	21.9	6.80	10.9	0.509	1170	0.056
0.221	0.0138	27.8	6.41	11.6	0.494	1210	0.061
0.217	0.0139	34.4	6.07	12.3	0.479	1240	0.066
0.201	0.0130	44.2	5.71	13.1	0.466	1290	0.072
			FLT 4 $M_\infty \approx 19$				
0.647	0.0469	1.23	10.50	2.86	1.05	631	0.030
0.573	0.0405	2.11	10.19	4.30	0.839	761	0.033
0.455	0.0313	3.67	9.57	5.91	0.705	881	0.036
0.330	0.0221	6.90	8.61	7.78	0.608	1000	0.040
0.318	0.0211	9.06	8.15	8.54	0.579	1040	0.042
0.305	0.0202	12.0	7.67	9.29	0.553	1090	0.045
0.251	0.0165	16.0	7.20	10.1	0.529	1130	0.048
0.249	0.0165	21.1	6.74	10.8	0.510	1170	0.052
0.218	0.0144	28.4	6.28	11.7	0.491	1210	0.057
0.193	0.0130	37.0	5.89	12.6	0.476	1260	0.062
0.164	0.0112	48.1	5.53	13.6	0.459	1320	0.068

the body is coupled to the inviscid flowfield by a streamtube mass balance. Effects of entropy-layer swallowing and body surface pressure overexpansion that result from the blunted nosetip are included. Air in thermodynamic equilibrium was assumed in this analysis. The momentum-thickness Reynolds number $Re_{e\theta}$ was evaluated by an integration along the cone, taking into consideration the streamwise variation of the boundary-layer edge properties due to the variable entropy and static pressure. The cone surface enthalpy h_w was determined by a coupled solution between aerodynamic heating and transient heat-conduction calculations.

V. Discussion

The base pressure data in Fig. 2 display the expected decrease with increasing Re_{∞_L} observed for slightly blunted slender cones at hypersonic Mach numbers.[8,13,14] For the present data, the base pressure ratio appears relatively insensitive to Mach number variations for $16 < M_\infty < 20$. Note that the wall-to-total-enthalpy ratio is essentially constant ($h_w/h_\infty \approx 0.04$) among all of the flights.

Data Comparisons

A comparison of the present data with limited full-scale RV flight data for slender cones[24-26] is presented in Fig. 3. For each flight, the data reveal the strong Reynolds-number dependence typical of the laminar-flow regime. These data are in general agreement for $M_\infty = 16$-22, despite differences in external configuration (θ_c and base geometry) and base radial location (R/R_B). In addition, note that various heatshield materials are represented in this data comparison (the present vehicles may be considered as nonablating for the range of Re_{∞_L} of interest). However, no definitive mass-addition effects due to heatshield ablation are discernible in Fig. 3. This observation is consistent with the flight data for slender cones with domed (hemisphere) afterbodies[26] for which no clear mass-addition trend was established in laminar flow.

The present flight data are plotted in terms of $M_\infty^2 Re_{\infty_S}^{-1/2}$ (from Kavanau[33]) in Fig. 4, together with available ground-test data[8,10-14] for the base centerline of slightly blunted ($R_N/R_B = 0.05$-0.10) slender cones at zero angle of attack (no sting-supported-model data are included). All of the ground-test data are for flat-based models, except the single data point of Cassanto et al.[11] for an 8.6° cone.† The flight data display general agreement with the bulk of the ground-test results, although there has been no attempt to include effects of variable h_w/H_∞ and test gas composition (γ) which characterize some of the ground-test data, as well as real-gas effects present in the flight data. Reeves and Buss[23] indicate that increasing h_w/H_∞ tends to increase the base pressure of a slender cone in laminar hypersonic flow, whereas the effect of including real-gas properties has been shown by Ohrenberger and Baum[24] to reduce substantially the laminar base pressure of slender RVs.

Data Correlations

Correlations Utilizing Freestream Conditions

Various freestream parameters have been proposed for correlating ground-test p_b/p_∞ data for sharp bodies.[9,33,36] While a correlation parameter based upon freestream properties can be misleading in the analysis of blunt-body data, an initial investigation in terms of freestream conditions provides some insight into the trends exhibited by the present data and establishes a basis for a more detailed discussion of these data. Because the RVs were nearly identical in both sphere-cone and base geometry, and since all data were obtained at a common base radial location, the applicability of freestream correlation parameters is somewhat strengthened. The fact that all data were measured at $R/R_B = 0.1$ is significant because severe radial gradients are characteristic of laminar base pressure, particularly at low Reynolds numbers.[7,10,13,14,16,19-21,23,25,33]

There has been some success in correlating sharp-cone ground-test p_b/p_∞ data with the parameter $M_\infty^n Re_{\infty_S}^{-1/2}$, where $n = 2$ or 3.[9,33] However, as seen in Fig. 4, considerable scatter is introduced into the flight data when plotted in terms of $M_\infty^2 Re_{\infty_S}^{-1/2}$. The correlation parameter $M_\infty^3 Re_{\infty_S}^{-1/2}$ (from Murman[9]) yields similar results for these data as well as for flight data[24,25] for 8° and 10° cones. It was also observed[27] that the flight p_b/p_∞ data fall considerably below the data level of the sharp cones correlated by Murman. This behavior is attributed to the generally higher h_w/H_∞ typical of the ground-test results,[23] real-gas effects present in the flight data,[24] and the effects of slight nose bluntness (particularly at high Reynolds numbers). Indeed, primarily because of entropy-layer swallowing, the present vehicles ($R_N/R_B \approx 0.05$) cannot be considered aerodynamically sharp for laminar boundary-layer flow in the range $2.5 \times 10^5 < Re_{\infty_L} < 4.8 \times 10^7$. Slight nose bluntness greatly affects the

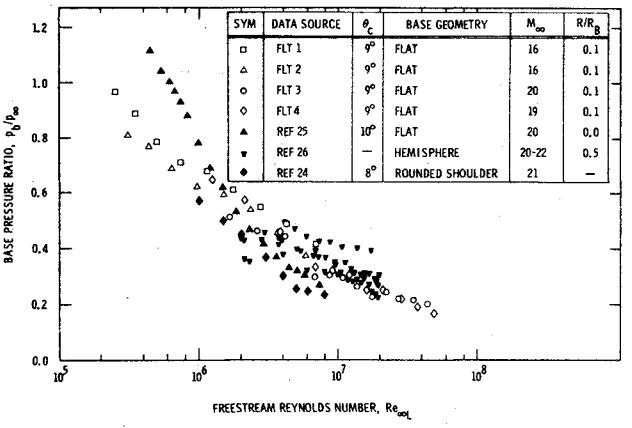

Fig. 3 Comparison of laminar hypersonic flight-test data.

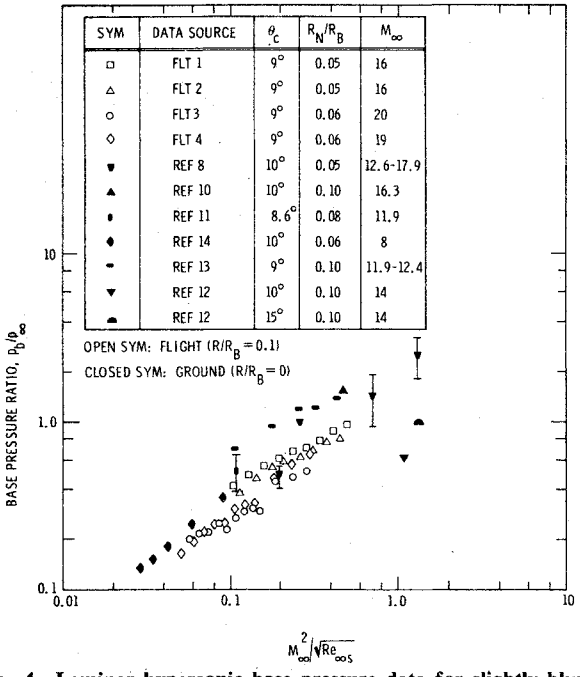

Fig. 4 Laminar hypersonic base pressure data for slightly blunted slender cones in terms of $M_\infty^2 Re_{\infty_S}^{-1/2}$.

†This data point represents the total variation in p_b/p_∞ for models with variable base geometry (ranging from flat to hemispherically-domed) and is shown for completeness. It is known that laminar base pressure is influenced by the base geometry, or more precisely, by the nature of boundary-layer separation preceding the base.[11,34,35]

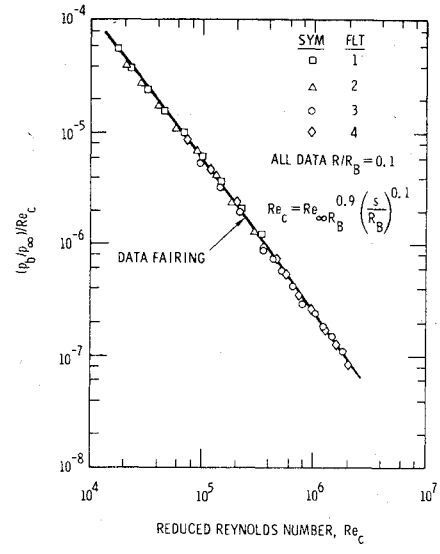

Fig. 5 Correlation of flight data with reduced Reynolds number.

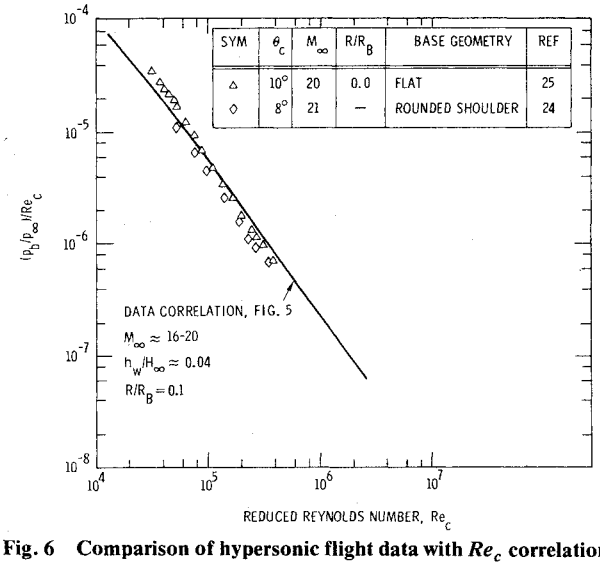

Fig. 6 Comparison of hypersonic flight data with Re_c correlation.

local cone boundary-layer edge properties[37,38] that should, in turn, influence the near-wake flowfield. The effects of slight nose bluntness on the present flight base pressure data are discussed in more detail later.

A base pressure correlation technique for general separated flows, which employs the reduced Reynolds number Re_c, has been used successfully by Wu and Su[36] to correlate supersonic ($2<M_\infty<5$) data for two-dimensional rearward facing steps and a two-dimensional wedge with laminar flow on the body preceding the separation point (i.e., the base). For a cone with axisymmetric laminar flow, the reduced Reynolds number assumes the form

$$Re_c = Re_{\infty R_B}^{0.9}(s/R_B)^{0.1} \tag{1}$$

where the base radius R_B is synonymous with the step height and the cone surface wetted length s is synonymous with the body length upstream of the separation point. It is noted that the Weiss model[39] indicates the base radius to be the length scale that controls base pressure for intermediate Reynolds numbers.

The reduced Reynolds number, Eq. (1), was applied to the present hypersonic data ($s/R_B \approx 6.1$), and the results are shown in Fig. 5. The excellent correlation of the parameter $(p_b/p_\infty)/Re_c$ with Re_c was somewhat unexpected because: 1) Re_c is independent of M_∞ (yet no Mach number effect is evident when the data are presented in this form); and 2) the vehicles were not aerodynamically sharp in laminar flow. The applicability of this correlation parameter in hypersonic flow appears to be substantiated by the present flight data, and Fig. 5 provides an efficient procedure for estimating base pressure near the centerline of similarly shaped vehicles. For example, agreement with other hypersonic flight data[24,25] is seen in Fig. 6. In general, however, note that plotting data in the manner suggested by Wu and Su may mask important base pressure variations. For the present flights, changes in p_b/p_∞ (of a factor of six) are dominated by a Reynolds-number variation of nearly three orders of magnitude. Thus, while the present correlation (Fig. 5) appears satisfactory, the results presented in both Figs. 5 and 6 may reflect the insensitive nature of the correlation method of Wu and Su.

Correlations Utilizing Local Conditions

The use of local cone properties immediately preceding the base (i.e., the boundary-layer edge properties at s) in correlating base pressure data has been demonstrated by many investigators (Cassanto, Rasmussen, and Coats[18] cite a number of examples from the literature). Correlations based on local cone properties provide a basis for comparing data for configurations differing from the present vehicles. For sharp cones, freestream parameters usually provide satisfactory correlations because unique relations exist between the local cone flow and the freestream conditions for a particular θ_c. However, for other geometrical shapes (e.g., spherically blunted cones), the variations of local Mach number M_e, local Reynolds number Re_{es}, and so forth (which are not uniquely related to the freestream conditions), play an important role in defining the near-wake flowfield and have, therefore, a definite influence on the base pressure.

It should be observed that the local cone properties computed for the present flight vehicles exhibit substantial deviations from "sharp-cone" flow (refer to Table 2). This circumstance is due to the presence of a bluntness-induced entropy layer and pressure variation along the vehicle which in turn produce streamwise variations in all of the boundary-layer edge properties. For low Re_{∞_L} (high altitudes), the flow is characteristic of a sharp 9° cone at constant M_∞, where $M_e \approx$ constant and $Re_{eL} > Re_{\infty_L}$. However, as Re_{∞_L} increases, significant variations occur in the local properties. For example, the variation of M_e for constant M_∞ is caused primarily by entropy-layer (or shock-curvature) effects introduced by the slight nose bluntness and becomes more pronounced with increasing freestream Reynolds number.[37,38] The nose-bluntness effects are very pronounced for Flights 3 and 4, which experienced generally higher freestream Reynolds numbers; for the largest Reynolds numbers, M_e is reduced by a factor of two and $Re_{eL} < Re_{\infty_L}$. These local property variations are significant despite the geometrical similarity of the four vehicles. For example, the higher freestream Mach numbers for Flights 3 and 4 are generally overshadowed by the effects of slight nose bluntness at high Reynolds numbers that tend to decrease the local Mach numbers far below those for Flights 1 and 2.

The effects of variable M_e, Re_{es}, etc. on the base pressure of a slender cone have been examined in a number of investigations.[6,7,12,17,18,23,40-42] Lien's analysis[40] of the data presented in Ref. 14 indicates that the base pressure ratio p_b/p_∞ decreases with increasing Re_{es} and decreasing M_e. In addition, Martellucci[41] correlated laminar data (no sting-supported models) with M_e and Re_{es} for a wider range of sphere-cone geometry ($5° < \theta_c < 15°, 0 < R_N/R_B < 0.3$) and freestream conditions ($M_\infty \approx 4$-19); this correlation reveals similar trends. Lockman[12] also considered the effects of local Mach number and local Reynolds number on base pressure in laminar hypersonic flow. For several free-flight models ($\theta_c = 10°$ and $15°, 0 < R_N/R_B < 0.5$) with constant h_w/H_∞, the

base-to-local-cone-pressure ratio p_b/p_e varied with M_e and Re_{es} as previously discussed and was correlated in terms of $M_e Re_{es}^{-1/2}$.

These trends were, in general, observed in the present data (Table 2). Several examples of analyses in terms of M_e and Re_{es} are presented in Ref. 27. However, attempts to correlate the flight data with ground-test results, solely in terms of M_e and Re_{es}, met with little success, probably because the higher h_w/H_∞ characteristic of ground-test data is not considered in any of these correlations. Apparently, the effects of cone-surface heat transfer (i.e., h_w/H_∞) should also be included for meaningful data comparisons, particularly if flight-test data are to be correlated with ground-test results. For example, the theoretical base pressure has been shown by Reeves and Buss[23] to depend upon the local cone properties (including h_w/H_∞ effects) in the following manner:

$$\frac{p_b}{p_e} \sim \left[\frac{M_e(1+\tfrac{1}{2}(\gamma-1)M_e^2)^{3/2}(1+4h_w/H_\infty)^{3/2}}{Re_{eR_B}}\right]^{1/2} \quad (2)$$

Note that the influence of the various local parameters on the base pressure is consistent with the previous discussion, although the theory for $M_e^2 \gg 1$ reveals a stronger Mach number effect ($p_b/p_e \sim M_e^2$) than that indicated, for example, by Lockman[12] (where $p_b/p_e \sim M_e$). The direct effect of the base radius R_B on the base pressure is also noted. This dependence was observed in the reduced Reynolds number (Figs. 5 and 6) and is discussed by Weiss.[39] Data correlations in terms of Eq. (2) are useful for predicting the base pressure of various geometrical configurations and have been used for example, for very blunt, high-drag planetary entry probes.[43]

The flight data are compared in Fig. 7 with sharp-cone ground-test data in terms of the Reeves and Buss correlation parameters. Both the flight- and ground-test results are correlated adequately over a large range of conditions, although a slope of 0.4 appears to fit all of the data better than does the value of 0.5 suggested by Reeves and Buss.‡ In particular, the present data are in close agreement with ground-test results when h_w/H_∞, real-gas, and nose-bluntness effects are included in the data comparison. Applications using these results are discussed in Sec. VI.

The Reynolds number based on some characteristic boundary-layer thickness parameter (e.g., total boundary-layer thickness δ or momentum thickness θ) has been considered in base pressure data analyses. Data[18] obtained from free flight models ($\theta_c = 10°, 0 < R_N/R_B < 0.6$) for a wide range of freestream conditions ($M_\infty = 4$-19, $Re_{\infty_L} = 4\times10^4$ to 3×10^6) indicate that, for the larger Reynolds numbers typical of hypersonic entry, the base pressure ratio decreases with increasing $Re_{e\delta}$ for constant M_e. Results from Lehnert and Schermerhorn[42] for sharp and blunt 10° cones indicate that for constant M_e and h_w/H_∞ the laminar base pressure ratio is a function of $Re_{e\theta}^{-1/2}$. This same variation with $Re_{e\theta}$ is observed in hypersonic base pressure data free of support-interference effects. Figure 8 presents a compilation of centerline data for sharp, flat-based 9° and 10° cones;[7,13,14,17,18,20-22] the bulk of the data is for 10° cones and reveals that the $Re_{e\theta}^{-1/2}$ dependence is generally valid for each group of hypersonic data corresponding to constant M_∞ or M_e.

A similar correlation of the present data in terms of $Re_{e\theta}$ is shown in Fig. 9. As indicated in Table 2, M_e varied for each flight at constant M_∞; therefore, only those data corresponding to approximately constant local Mach number ($M_e = 9.5$-10.5) are included in Fig. 9. However, the remaining data in Table 2, when compared to the $M_e \approx 10$ data plotted in Fig. 9, clearly reveal the effect of slight nose bluntness on the base pressure. For essentially constant $Re_{e\theta}$ ($\sim$1000-1300), the base pressure ratio is reduced significantly as M_e is

‡For a sharp cone at constant M_∞, Re_{eL} is proportional to Re_{∞_L} (perfect gas). This indicates, therefore, that $p_b/p_\infty \sim Re_{\infty_L}^{-0.4}$.

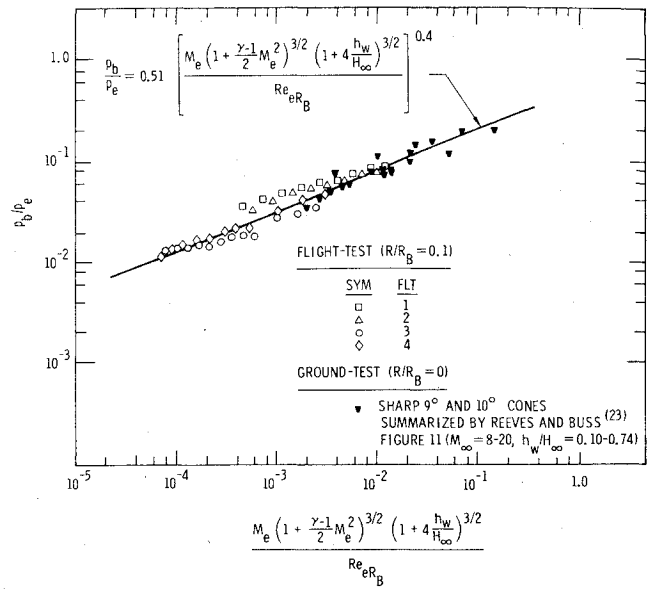

Fig. 7 Data correlation utilizing local parameters from the Reeves and Buss theory.

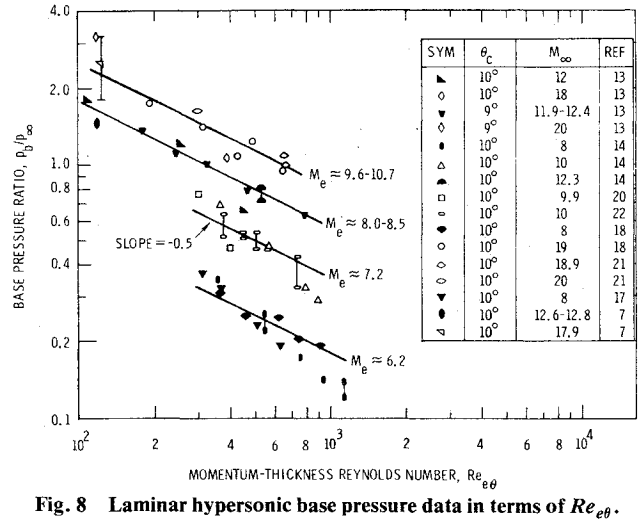

Fig. 8 Laminar hypersonic base pressure data in terms of $Re_{e\theta}$.

decreased below $M_e \approx 10$; for example, p_b/p_∞ for Flights 3 and 4 is reduced by approximately 50% for the lowest values of M_e ($M_e \approx 5.6$). This data correlation provides additional evidence of the influence of slight nose bluntness on the base pressure and indicates that $Re_{e\theta}^{-1/2}$ is a proper correlating variable for a particular configuration providing M_e and h_w/H_∞ are relatively constant. Note that in terms of $Re_{e\theta}$, the present $M_e \approx 10$ flight data reveal a significant reduction from the ground-test data level (Fig. 8) for corresponding Mach numbers (i.e., $M_e \approx 9.6$-10.7). As discussed earlier, this trend is consistent with the lower h_w/H_∞ characteristic of full-scale RV re-entry conditions.

VI. Applications

As indicated in the Introduction, this study is primarily directed toward establishing a semi-empirical capability for re-entry vehicle preflight predictions and postflight data analyses. Data correlations in terms of local parameters provide the greatest flexibility for developing a basis for such computations. A brief investigation of several slender cones is included herein to illustrate, for example, real-gas and nose-bluntness effects on the base pressure of full-scale re-entry vehicles in laminar hypersonic flow.

For the purpose of this analysis, the correlation shown in Fig. 7 in terms of the Reeves and Buss correlation parameters

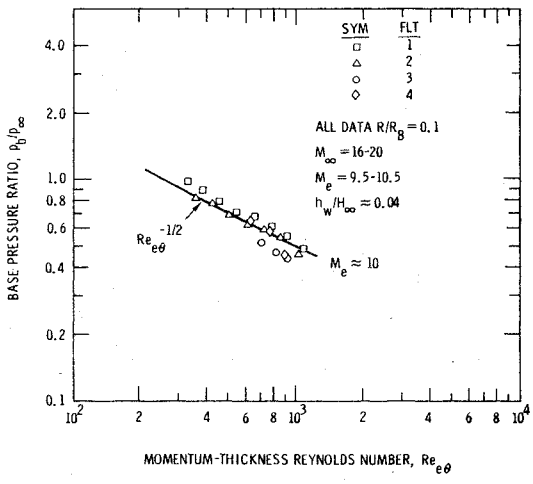

Fig. 9 Correlation of flight data with $Re_{e\theta}$ ($M_e \approx 10$).

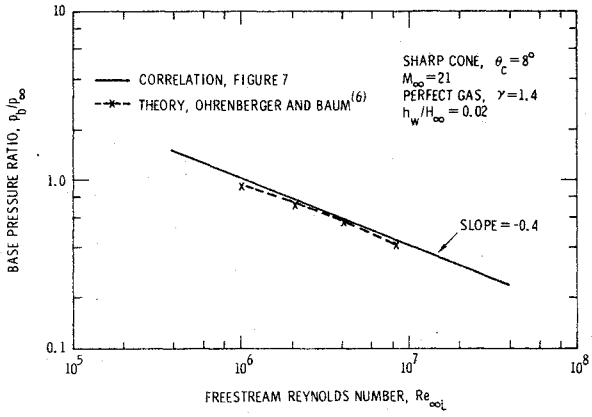

Fig. 10 Base pressure prediction for sharp 8° cone.

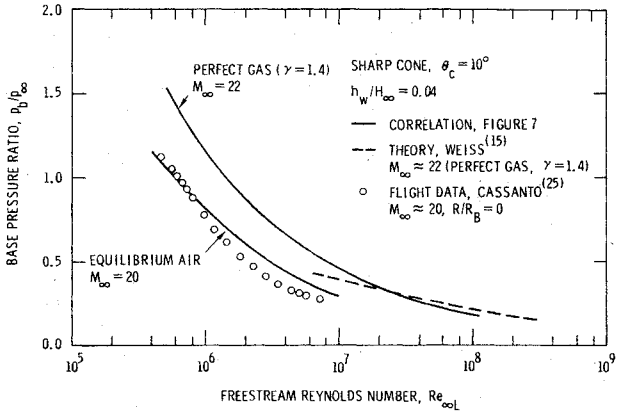

Fig. 11 Predictions for sharp 10° cones and comparison with flight data.

is considered. While other correlation parameters could be utilized here, it is felt that Fig. 7 represents an accurate approach to the evaluation of base pressure for other configurations because: 1) the correlation parameters were derived from theory; and 2) the present data were adequately correlated with ground-test data in terms of these parameters. Strictly speaking, because of the radial base pressure gradients usually present in laminar flow,[7,10,13,14,16,19-21,23,25,33] this correlation is applicable only in the vicinity of the base centerline ($0 < R/R_B < 0.2$). Generally, very little deviation in p_b/p_∞ from the centerline value is observed in this region for data free of support-interference effects.[10,13,14,16,20,21]

Estimation of p_b/p_∞ based upon Fig. 7 for the centerline of a sharp 8° cone at $M_\infty = 21$ is presented in Fig. 10 as a function of the freestream Reynolds number. This prediction is for a cold wall ($h_w/H_\infty = 0.02$), and a perfect gas ($\gamma = 1.4$) is assumed. These calculations are compared with the theory of Ohrenberger and Baum[6] for a perfect gas, and both the levels and slopes of the base pressure curves show good agreement.

Further application of the correlation for the centerline of a sharp 10° cone is shown in Fig. 11. Two calculations based upon Fig. 7 are provided. The first is for $M_\infty = 22$ and is presented for comparison with theoretical results; a perfect gas ($\gamma = 1.4$) and $h_w/H_\infty = 0.04$ are assumed. This calculation is compared with the theory of Weiss[15] (perfect gas) for atmospheric entry at $V_\infty = 22{,}000$ fps ($M_\infty \approx 22$) and $h_w/H_\infty = 0.04$. Reasonably good agreement is seen between the perfect-gas calculation and theory for high Reynolds numbers where the theory is applicable.

Full-scale RV flight data[25] for a 10° cone at $M_\infty \approx 20$ shown in Fig. 11 are well below both the perfect-gas calculation and theory. Utilization of real-gas properties has been shown by Ohrenberger and Baum[24] to reduce substantially the base pressure of slender RVs in laminar flow. The second calculation based upon Fig. 7 includes real-gas properties (equilibrium air) and is provided for comparison with the flight data at $M_\infty = 20$. Note that with the assumption of equilibrium air the calculations are brought into better agreement with the flight data. While part of the reduction in the calculated base pressure ratio is due to the lower Mach number ($M_\infty = 20$ instead of 22), the primary influence is the effect of real-gas properties in the evaluation of the local cone Reynolds numbers. Introduction of equilibrium air into the local cone calculations[32] results in an increase in the local cone Reynolds numbers compared with corresponding perfect-gas values. These larger Reynolds numbers effectively "thin" the boundary layer immediately preceding the base and thus reduce the base pressure as given by Fig. 7. This reduction is significant for the 10° cone in Fig. 11 (for example, p_b/p_∞ is reduced by approximately 35% at $Re_{\infty_L} = 10^6$) and is comparable to that reported at $M_\infty = 21$ for an 8° cone.[24]

Figures 10 and 11 illustrate the utility and reliability of a correlation based upon local cone properties. Figure 7 appears to be adequate for predicting the base pressure of sharp, slender configurations in hypersonic entry conditions. However, because even slight nose bluntness can produce substantial variations in the local cone properties (particularly at high Reynolds numbers), it is meaningful to briefly investigate the effects of nose bluntness on the base pressure of a slender cone in laminar flow.

A 5-ft-long, spherically blunted 7° cone was chosen for this study. The assumed flow conditions are typical of hypersonic entry ($M_\infty = 20$ and $h_w/H_\infty = 0.02$). Several values of bluntness ratio were considered, 0.0 (sharp), 0.05, 0.10, and 0.20. The local cone properties for laminar flow were determined with the procedure[32] utilized in the analysis of the present flight data; entropy-layer swallowing and body surface pressure overexpansion were considered, and all computations were performed assuming equilibrium air. Note that the calculations are length-dependent: together with θ_c and R_N/R_B, the specification of the body length L (or the nose radius R_N) is required to compute the local cone properties for a spherically blunted cone. As discussed earlier, this is particularly true for slightly blunted cones in laminar hypersonic flow, for which the bluntness-induced entropy layer and pressure variation along the vehicle produce significant streamwise variations in all of the boundary-layer edge properties.

Results for the 7° cones are plotted in Fig. 12 for $Re_{\infty_L} = 10^5$ to 10^8. This parametric study reveals that, for a given Re_{∞_L}, increasing R_N/R_B substantially reduces p_b/p_∞. Also, for a fixed R_N/R_B, the effect of nose bluntness is aggravated by an increasing freestream Reynolds number; as expected, even slight nose bluntness influences the base pressure at high Reynolds numbers. For example, p_b/p_∞ at $Re_{\infty_L} = 10^8$ is

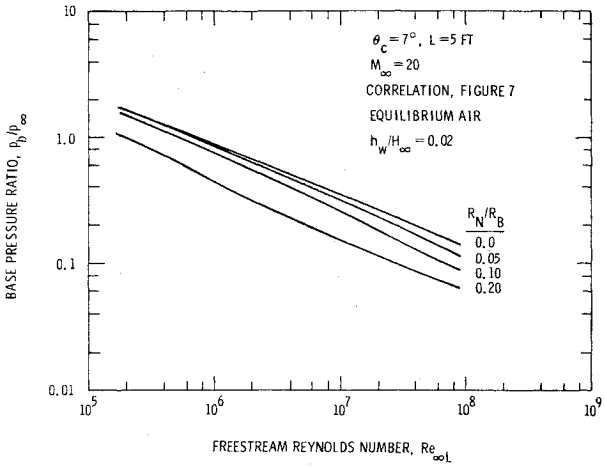

Fig. 12 Effect of nose bluntness on base pressure of a slender cone.

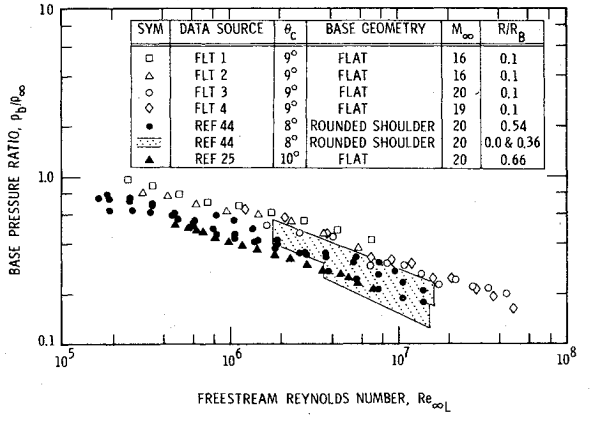

Fig. 13 Comparison of present results with data of Batt and Cassanto.

reduced from the corresponding sharp-cone value by 25% for 0.05 bluntness and by 40% for 0.10 bluntness. This identical behavior (i.e., the effect of slight nose bluntness at high Re_{∞_L} decreasing the base pressure) was observed in the present flight data. Since the viscous boundary-layer flow over most RVs is affected to some extent by nose bluntness, the implications in full-scale flight tests are obvious.

The parametric studies provided in Figs. 11 and 12 demonstrate the importance of real-gas and nose-bluntness effects in evaluating the base pressure of a slender cone. The applicability of the correlations of the present data appears to be substantiated by both data and theory for several slender cones in laminar hypersonic flow; further verification of other configurations awaits additional flight results. Flight tests of both slightly blunted and relatively blunt, slender re-entry vehicle configurations are currently in progress.

VII. Addendum

Following preparation of this manuscript, a related paper by Batt[44] subsequently became available to the author. This recent investigation describes laminar base pressure measurements on a number of slender conical re-entry vehicles at $M_\infty = 20$.

The data compiled by Batt are for 8° cones with rounded shoulder bases and $R_N/R_B < 0.02$. These results are compared in Fig. 13 with the present data for 9° cones in terms of the freestream Reynolds number. Data for the 8° cones include measurements at several radial locations: $R/R_B = 0.0$, 0.36, and 0.54 (the data at $R/R_B = 0.0$ and 0.36 are grouped to summarize the collected results for several flights).§ Also shown are additional flight data at $R/R_B = 0.66$ from Cassanto[25] for the 10° cone previously discussed.

A comparison of the data shown in Fig. 13 reveals the expected radial gradient in the base pressure; for low Reynolds numbers, those data corresponding to the largest R/R_B display the lowest base pressure ratios. Note that all of the data indicate approximately the same variation (i.e., slope) with Re_{∞_L}. Batt's comparison of the 8° cone data with the $p_b/p_\infty - Re_{\infty_L}$ slope predicted by Ohrenberger and Baum[6] indicates favorable agreement. In addition, as shown in Fig. 10, the analytical results of Ohrenberger and Baum agree closely with the Reynolds-number slope of -0.4 given by the present data analysis. As noted by Batt and as observed earlier by the author, the general agreement between data for slender cones with slightly different θ_c is to be expected for laminar hypersonic flow conditions.

§During review of this paper it was brought to the author's attention that Batt's results for $R/R_B = 0.54$ include the data discussed by Ohrenberger and Baum.[24]

VIII. Summary and Conclusions

Base pressure data obtained from four slightly blunted slender-cone re-entry vehicles have been compared with available theory and ground- and flight-test data for similar configurations. The present data for $M_\infty \approx 16$-20 reveal the expected dependence on Reynolds number for Re_{∞_L} from 2×10^5 to 5×10^7 in laminar hypersonic flow and, in general, show good agreement with other hypersonic flight data. General agreement with ground-test results was also observed, taking into consideration differences due to variable test gas composition, different wall-to-total-enthalpy ratio, and real-gas and nose-bluntness effects. The flight data indicate a strong influence of slight nose bluntness at high Reynolds numbers; this behavior is attributed to local cone boundary-layer edge property variations resulting from entropy-layer (or shock-curvature) effects.

The base pressure data correlated well with the reduced Reynolds number proposed by Wu and Su. This correlation provides a prediction procedure for RVs similar to those considered here. Correlations in terms of local cone (boundary-layer edge) conditions were also considered in view of the objective of developing a prediction capability for other RV configurations in hypersonic entry conditions. A correlation of the present data with ground-test results was found in terms of the theoretically-derived parameters from Reeves and Buss. Finally, sharp- and blunt-cone base pressure data were investigated in terms of the momentum-thickness Reynolds number; these data as well as the present flight data indicate that $Re_{e\theta}^{1/2}$ is a proper correlating variable in laminar hypersonic flow.

The local-property correlation in terms of the Reeves and Buss parameters was utilized to calculate the base pressure of 7°, 8°, and 10° cones. This investigation revealed strong real-gas effects on laminar base pressure in hypersonic flow and supports the theory of Ohrenberger and Baum. Perfect-gas predictions for 8° and 10° cones showed generally good agreement with the theory of Ohrenberger and Baum and of Weiss, and agreement was seen between the 10° cone calculation assuming equilibrium air and full-scale RV flight data from Cassanto. A parametric study for 7° cones indicated substantial reductions in base pressure due to nose bluntness which was observed in the present flight data for slightly blunted cones. It is concluded that flight-data correlations represent a practical approach to evaluation of the base pressure of slender re-entry configurations in laminar hypersonic flow.

References

[1] Lees, L., "Hypersonic Wakes and Trails," *AIAA Journal*, Vol. 2, March 1964, pp. 417-428.

[2] Lykoudis, P. S., "A Review of Hypersonic Wake Studies," *AIAA Journal*, Vol. 4, April 1966, pp. 577-590.

[3] Proceedings, AGARD Specialists Meeting, *Fluid Physics of Hypersonic Wakes*, Vols. 1 and 2, AGARD CP 19, May 1967, Colorado State University, Fort Collins, Colo.

[4]Chang, P. K., *Separation of Flow*, 1st ed., Pergamon Press, New York, 1970, Chapts. 8, 10 and 11.

[5]Berger, S. A., *Laminar Wakes*, Elsevier, New York, 1971.

[6]Ohrenberger, J. T. and Baum, E., "A Theoretical Model of the Near Wake of a Slender Body in Supersonic Flow," *AIAA Journal*, Vol. 10, Sept. 1972, pp. 1165-1172.

[7]Softley, E. J., Muntz, E. P., and Zempel, R. E., "Experimental Determination of Pressure, Temperature, and Density in Some Laminar Hypersonic Near Wakes," TIS R64SD35, May 1964, Space Sciences Lab., General Electric Co., Philadelphia, Pa.

[8]Muntz, E. P. and Softley, E. J., "A Study of Laminar Near Wakes," *AIAA Journal*, Vol. 4, June 1966, pp. 961-968.

[9]Murman, E. M., "Experimental Studies of a Laminar Hypersonic Cone Wake," *AIAA Journal*, Vol. 7, Sept. 1969, pp. 1724-1730.

[10]Peterson, C. W., "An Experimental Study of Laminar Hypersonic Blunt Cone Wakes," *Astronautica Acta*, Vol. 15, Dec. 1969, pp. 67-76.

[11]Cassanto, J. M., Schiff, J., and Softley, E. J., "Base Pressure Measurements on Slender Cones with Domed Afterbodies," *AIAA Journal*, Vol. 7, 1969, pp. 1607-1609.

[12]Lockman, W. K., "Free-Flight Base Pressure and Heating Measurements on Sharp and Blunt Cones in a Shock Tunnel," *AIAA Journal*, Vol. 5, Oct. 1967, pp. 1898-1900.

[13]Softley, E. J. and Graber, B. C., "An Experimental Study of the Pressure and Heat Transfer on the Base of Cones in Hypersonic Flow," *Fluid Physics of Hypersonic Wakes*, Vol. 1, AGARD CP 19, May 1967.

[14]Martellucci, A., Ranlet, J., Schlesinger, A., and Garberoglio, J., "Experimental Study of Near Wakes, Volume I—Data Presentation," GASL TR-641-Vol. I (BSD-TR-67-229-Vol. I), Nov. 1967, General Applied Science Lab., Inc., Westbury, N.Y.

[15]Weiss, R., "The Near Wake of a Cone," AERL 65-2979, Research Note 586 (BSD-TR-65-474), Oct. 1965, AVCO-Everett Research Lab., Everett, Mass.

[16]Zakkay, V. and Cresci, R. J., "An Experimental Investigation of the Near Wake of a Slender Cone at $M_\infty = 8$ and 12," *AIAA Journal*, Vol. 4, Jan. 1966, pp. 41-46.

[17]Schmidt, E. M., "An Investigation of Hypersonic Flow Around a Slender Cone," *AIAA Student Journal*, Vol. 3, Dec. 1965, pp. 129-133.

[18]Cassanto, J. M., Rasmussen, N. S., and Coats, J. D., "Correlation of Free-Flight Base Pressure Data for $M = 4$ to $M = 19$," *AIAA Journal*, Vol. 7, June 1969, pp. 1154-1157.

[19]Miller, C. G., III, "Experimental Base Pressures on 9° Spherically Blunted Cones at Mach Numbers from 10.5 to 20," TN D-4800, Oct. 1968, NASA.

[20]Pick, G. S., "Base Pressure Distribution of a Cone at Hypersonic Speeds," *AIAA Journal*, Vol. 10, Dec. 1972, pp. 1685-1686.

[21]Cassanto, J. M., "Free Flight Base Pressure Results for a Sharp Cone at Angle of Attack," ALDM 70-78, March 1970, Re-entry and Environmental Systems Div., General Electric Co., Philadelphia, Pa.

[22]Ward, L. K. and Choate, R. H., "A Model Drop Technique for Free-Flight Measurements in Hypersonic Wind Tunnels Using Telemetry," AEDC-TR-66-77, May 1966, Arnold Engineering Development Center, Tullahoma, Tenn.

[23]Reeves, B. L. and Buss, H. M., "Theory of the Laminar Near Wake of Axisymmetric Slender Bodies in Hypersonic Flow," AVMSD-0122-69-RR, Feb. 1969, AVCO Missile Systems Div., Wilmington, Mass.

[24]Ohrenberger, J. T. and Baum, E., "Laminar Near Wake Solutions Under Atmospheric Entry Conditions," AIAA Paper 72-116, San Diego, Calif., 1972.

[25]Cassanto, J. M., "Radial Base-Pressure Gradients in Laminar Flow," *AIAA Journal*, Vol. 5, Dec. 1967, pp. 2278-2279.

[26]Cassanto, J. M. and Hoyt, T. L., "Flight Results Showing the Effect of Mass Addition on Base Pressure," *AIAA Journal*, Vol. 8, Sept. 1970, pp. 1705-1707.

[27]Bulmer, B. M., "Correlation of Reentry Base Pressure in Laminar Hypersonic Flow," SLA-74-0169, Aug. 1974, Sandia Labs., Albuquerque, N. Mex.

[28]Wilson, L. N., "Body-Shape Effects on Axisymmetric Wakes: Transition," *AIAA Journal*, Vol. 4, Oct. 1966, pp. 1741-1747.

[29]Waldbusser, E., "Geometry of the Near Wake of Pointed and Blunt Hypersonic Cones," *AIAA Journal*, Vol. 4, Oct. 1966, pp. 1874-1876.

[30]Cassanto, J. M., "A Method of Determining Onset of Boundary Layer Transition from Flight Test Base Pressure Data," ATFM 67-23, Oct. 1967, Re-entry Systems Dept., General Electric Co., Philadelphia, Pa.

[31]Bulmer, B. M., "Detection of Flight Vehicle Transition from Base Measurements," *Journal of Spacecraft and Rockets*, Vol. 10, April 1973, pp. 280-281.

[32]Hochrein, G. J., "A Procedure for Computing Aerodynamic Heating on Sphere Cones—Program BLUNTY," SC-DR-69-449, Nov. 1969, Sandia Labs., Albuquerque, N. Mex.

[33]Kavanau, L. L., "Base Pressure Studies in Rarefied Supersonic Flows," *Journal of the Aeronautical Sciences*, Vol. 23, March 1956, pp. 193-207.

[34]Weiss, R. F. and Weinbaum, S., "Hypersonic Boundary-Layer Separation and the Base Flow Problem," *AIAA Journal*, Vol. 4, Aug. 1966, pp. 1321-1330.

[35]Hama, F. R., "Experimental Studies on the Lip Shock," *AIAA Journal*, Vol. 6, Feb. 1968, pp. 212-219.

[36]Wu, J. M., Su, M. W., and Moulden, T. H. (The University of Tennessee Space Institute), "On the Near Flow Field Generated by the Supersonic Flow Over Rearward Facing Steps," ARL 71-0243, Nov. 1971, Aerospace Research Labs., Wright-Patterson Air Force Base, Ohio; and *AIAA Journal*, Vol. 9, July 1971, pp. 1429-1431.

[37]Rotta, N. R. and Zakkay, V., "Effects of Nose Bluntness on the Boundary Layer Characteristics of Conical Bodies at Hypersonic Speeds," *Astronautica Acta*, Vol. 13, Aug. 1968, pp. 507-516.

[38]Wilson, R. E., "Laminar Boundary-Layer Growth on Slightly Blunted Cones at Hypersonic Speeds," *Journal of Spacecraft and Rockets*, Vol. 2, July-Aug. 1965, pp. 490-496.

[39]Weiss, R. F., "Base Pressure of Slender Bodies in Laminar, Hypersonic Flow," *AIAA Journal*, Vol. 4, Sept. 1966, pp. 1557-1559.

[40]Lien, H., "Experimental Study of Near Wakes, Volume III—Correlation of Data and Simplified Methods for Predicting Some Base Flow Properties," GASL TR-641-Vol. III (BSD-TR-67-229, Vol. III), Nov. 1967, General Applied Science Labs., Inc., Westbury, N.Y.

[41]Martellucci, A., "Laminar Base Pressure Correlation," ATDM 67-13, March 1967, Re-entry Systems Department, General Electric Co., Philadelphia, Pa.

[42]Lehnert, R. and Schermerhorn, V. L., "Correlation of Base Pressure and Wake Structure of Sharp-and Blunt-Nose Cones With Reynolds Number Based on Boundary-Layer Momentum Thickness," *Journal of the Aero/Space Sciences*, Vol. 26, March 1959, pp. 185-186.

[43]Zappa, O. L. and Reinecke, W. G., "An Experimental Investigation of Base Heating on Typical Mars Entry Body Shapes," *Journal of Spacecraft and Rockets*, Vol. 10, April 1973, pp. 273-276.

[44]Batt, R. G., "Flight Test Base Pressure Results for Sharp 8° Cones," *AIAA Journal*, Vol. 12, April 1974, pp. 555-557.